STRUCTURAL BIOLOGY COMMUNICATIONS

ISSN 2053-230X

Received 19 January 2021
Accepted 23 March 2021

Edited by R. Sankaranarayanan, Centre for Cellular and Molecular Biology, Hyderabad, India

‡ These authors contributed equally to this work.

Keywords: hemoglobin; mouse; oxygen transport; oxygen storage; methemoglobin.

PDB reference: mouse hemoglobin, 3hrw

Supporting information: this article has supporting information at journals.iucr.org/f

Crystal structure of hemoglobin from mouse (*Mus musculus*) compared with those from other small animals and humans

Selvarajan Sigamani Sundaresan,[a]‡ Pandian Ramesh,[b]*‡ Nagaraj Shobana,[c] Thangaraj Vinuchakkaravarthy,[b] Sayed Yasien[b] and Mondikalipudur Nanjappa Gounder Ponnuswamy[d]*

[a]Department of Physics, Sir Theagaraya College, Chennai 600 021, India, [b]Protein Structure–Function Research Unit, School of Molecular and Cell Biology, University of the Witwatersrand, Braamfontein, Johannesburg 2050, South Africa, [c]Department of Physics and Industrial Electronics, Shrimati Indira Gandhi College, Tiruchirappalli 620 002, India, and [d]Centre of Advanced Study in Crystallography and Biophysics, University of Madras, Guindy Campus, Chennai 600 025, India. *Correspondence e-mail: prms23.crystal@gmail.com, mnpsy2004@yahoo.com

Mice (*Mus musculus*) are nocturnal small animals belonging to the rodent family that live in burrows, an environment in which significantly high CO_2 levels prevail. It is expected that mouse hemoglobin (Hb) plays an important role in their adaptation to living in such a high-CO_2 environment, while many other species cannot. In the present study, mouse Hb was purified and crystallized at a physiological pH of 7 in the orthorhombic space group $P2_12_12_1$; the crystals diffracted to 2.8 Å resolution. The primary amino-acid sequence and crystal structure of mouse Hb were compared with those of mammalian Hbs in order to investigate the structure–function relationship of mouse Hb. Differences were observed from guinea pig Hb in terms of amino-acid sequence and from cat Hb in overall structure (in terms of r.m.s.d.). The difference in r.m.s.d. from cat Hb may be due to the existence of the molecule in a conformation other than the R-state. Analysis of tertiary- and quaternary-structural features, the $\alpha1\beta2$ interface region and the heme environment without any ligands in all four heme groups showed that mouse methemoglobin is in an intermediate state between the R-state and the T-state that is much closer to the R-state conformation.

1. Introduction

Hemoglobin (Hb) is an allosteric protein that exists in an equilibrium between two alternative structures, the T- (tense) and R- (relaxed) states, which possess low and high oxygen affinity, respectively (Monod *et al.*, 1965). Transition from the T- to the R-state involves rotation and a shift of one of the dimers relative to the other symmetry-related dimers. This movement results in the disruption and/or the formation of new hydrogen bonds and salt bridges across the interface region of hemoglobin. Hydrogen bonds and salt-bridge interactions are more significant in the T-state structure when compared with the R-state structure.

The initial strategy developed by Perutz to grow liganded Hb crystals under high-salt conditions revealed the existence of the R-state (Perutz, 1968). The existence of multiple quaternary states (R2, RR2 and R3) of liganded Hbs has also been reported (Silva *et al.*, 1992; Mueser *et al.*, 2000; Safo & Abraham, 2001, 2005). The existence of multiple states provides clear evidence that the dimer–dimer interface of liganded Hb can adopt a wide range of energetically accessible structures that are related to each other by a simple sliding

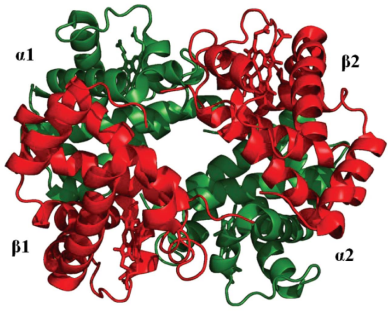

motion without greatly altering the number or the nature of inter-subunit contacts.

The gas composition in rodent burrows differs from that of environmental air, creating situations of potential respiratory difficulty for these fossorial mammals. Field observations of pocket gopher burrows have revealed CO_2 concentrations ranging from 0.6% to 3.8% and O_2 concentrations ranging from 6.0% to 14.0% (Kennerly, 1964; McNab, 1966). A maximum CO_2 concentration of 6% has been found in the burrows of thirteen-lined squirrels (*Spermophilus tridecemlineatus*), whereas the normal concentrations of CO_2 and O_2 in air are 0.04% and 20.95%, respectively (Studier & Procter, 1971). Circulation of air inside the burrows is poorly achieved by respiration of the rodents, while soil micro-organisms also account for the accumulation of a high concentration of CO_2 and depletion of O_2 in the burrows. With all of the above concepts in mind, we chose to compare the quaternary structure–function correlation of mouse Hb with those of human Hb and other small animal Hbs.

2. Materials and methods

2.1. Purification and crystallization

Mouse Hb was purified using previously reported procedures (Sundaresan *et al.*, 2009; Ramesh *et al.*, 2013). In brief, fresh blood collected from mice was mixed with 10%(*w*/*v*) ethylenediaminetetraacetic acid (EDTA) to avoid clotting. The red blood cells were isolated from the blood by centrifuging the sample at 5000 rev min^{-1} for 20 min at 4°C. The pellet was recovered and washed three times with two volumes of saline solution followed by hemolysis with the addition of Milli-Q water to three times the volume of the pellet. The hemolyzed solution was centrifuged at 10 000 rev min^{-1} for 1 h at 4°C, which yielded cell-free hemoglobin in the supernatant. Further purification was carried out by applying the supernatant onto a DEAE cellulose anion-exchange column pre-equilibrated with water at physiological pH (Knapp *et al.*, 1999). Material bound to the column was initially eluted with water, followed by stepwise elution with sodium chloride solution at various concentrations. A single peak was obtained at 0.1 *M* NaCl and was collected at a rate of 3 ml min^{-1}. A 10% native PAGE was carried out to confirm the homogeneity of the mouse hemoglobin (Davis, 1964). The concentration of Hb was estimated as 40 mg ml^{-1} using the Bradford absorption method at 595 nm (Bradford, 1976).

Mouse Hb was crystallized at 20°C using the hanging-drop vapor-diffusion method. Initially, the crystallization conditions were optimized by varying the concentration of protein using different precipitants such as MPD and PEG with molecular weight in the range 2000–8000. Diffraction-quality crystals of mouse Hb were obtained after a week by equilibrating 3 µl hemoglobin solution and 3 µl reservoir solution consisting of 35% PEG 3350 (Sigma) in water against 1 ml reservoir solution.

2.2. Data collection, processing, structure solution and refinement

A crystal of dimensions 0.3 × 0.25 × 0.2 mm was mounted in a cryo-loop with glycerol as a cryoprotectant and intensity data were collected at 100 K on a MAR345dtb image plate with a crystal-to-detector distance of 150 mm. The data were indexed, integrated, merged and scaled using the *AUTOMAR* and *SCALEPACK* software packages (Bartels & Klein, 2003). Structure solution was obtained by the molecular-replacement method with human hemoglobin (PDB entry 1hab; Schumacher *et al.*, 1997) as the search model using *Phaser* (McCoy *et al.*, 2007) as implemented in the *CCP*4 suite (Winn *et al.*, 2011). Structure refinement was performed by *REFMAC* (Murshudov *et al.*, 2011). The model obtained from structure solution was subjected to 20 cycles of rigid-body refinement followed by ten cycles of restrained refinement. At this stage, the electron-density map was calculated and the amino-acid sequence of human Hb was replaced with that of mouse Hb using *Coot* (Emsley *et al.*, 2010) where necessary, as shown in Supplementary Table S1. The refined structure was evaluated using a Ramachandran plot in *PROCHECK* (Laskowski *et al.*, 1993). The data-collection and refinement statistics for mouse Hb are listed in Table 1.

3. Results and discussion

3.1. The overall structure of mouse hemoglobin

The sequences and structures of human Hbs [oxy R-state Hb (PDB entry 1hho; Shaanan, 1983), carboxy R-state Hb (PDB entry 1aj9; Vásquez *et al.*, 1998), deoxy T-state Hb (PDB entry 2hhb; Fermi *et al.*, 1984) and met R2-state Hb (PDB entry 1jy7; Biswal & Vijayan, 2001)] and Hbs from other small animals such as brown rat (BRat) Hb (PDB entry 3hf4; K. Neelagandan, P. Sathya Moorthy, M. Balasubramanian & M. N. Ponnuswamy, unpublished work), deer mouse (DMouse) Hb [deoxy T-state (PDB entry 5ker; Inoguchi *et al.*, 2017) and aquo-met R-state (PDB entry 4h2l; Inoguchi *et al.*, 2013)], guinea pig (GPig) Hb [oxy form (PDB entry 3a0g; S. Etti, G. Shanmugam, P. Karthe & K. Gunasekaran, unpublished work) and met R2-state (PDB entry 3hyu; Pairet & Jaenicke, 2010)], mongoose oxy Hb (PDB entry 4yu4; M. M. Abubakkar, V. Maheshwaran & M. N. Ponnuswamy, unpublished work), American pika (APika) Hb (PDB entry 5eui; N. Inoguchi, C. Natarajan, J. F. Storz & H. Moriyama, unpublished work), rabbit oxy Hb (PDB entry 2rao; S. Sundaresan, C. Packianathan, K. Neelagandan & M. N. Ponnuswamy, unpublished work), European hare (EHare) oxy Hb (PDB entry 3lqd; P. Sathya Moothy, M. Thenmozhi, M. Balasubramanian & M. N. Ponnuswamy, unpublished work) and cat Hb (PDB entry 3gqp; B. Balasubramanian, P. Sathya Moorthy, K. Neelagandan & M. N. Ponnuswamy, unpublished work) were retrieved from the PDB. A multiple sequence alignment of the amino-acid sequences of both the α and β chains of all of the chosen Hbs was carried out using *Clustal Omega* (https://www.ebi.ac.uk/Tools/msa/clustalo) followed by a secondary-structure component prediction for the aligned sequences

Table 1
Data-collection, processing and refinement statistics for mouse Hb.

Values in parentheses are for the highest resolution shell.

Data-collection and processing statistics	
X-ray source	Cu $K\alpha$
Wavelength (Å)	1.5418
Temperature (K)	100
Oscillation angle (°)	1
Crystal-to-detector distance (mm)	150
Resolution (Å)	19.90–2.80 (2.90–2.80)
Space group	$P2_12_12_1$
Unit-cell parameters (Å)	a = 53.08, b = 65.94, c = 150.93
Observed/unique reflections	33641/12720
Matthews coefficient V_M (Å^3 Da^{-1})	2.11
Solvent content (%)	41.62
No. of molecules in asymmetric unit	1
R_{merge} (%)	11.35 (42.42)
$R_{p.i.m.}$ (%)	28.41 (62.37)
Multiplicity	2.61 (1.98)
Completeness (%)	93.0 (90.0)
Average $I/\sigma(I)$	2.8 (1.0)
Structure refinement	
Resolution limit (Å)	19.94–2.80
No. of reflections	11999
R factor/R_{free} (%)	24.26/30.56
R.m.s.d., bond lengths (Å)	0.011
R.m.s.d., bond angles (°)	1.572
R.m.s.d., chiral volumes (Å^3)	0.095
Mean B value (Å^2)	36.57
Ramachandran plot	
Residues in most favorable regions (%)	90.0
Residues in additional allowed regions (%)	8.6
Residues in generously allowed regions (%)	1.4
Residues in disallowed region (%)	0.0
PDB code	3hrw

based on the mouse Hb structure using *ESPript*3 (http://espript.ibcp.fr/ESPript/cgi-bin/ESPript.cgi; Robert & Gouet, 2014) as shown in Fig. 1; the percentile identity matrix is shown in Supplementary Table S2. The mouse and human Hbs share about 86% and 80% sequence identity for the α and β chains, respectively. The percentage sequence identities of mouse Hb to other small animal Hbs are similar, except for GPig Hb, which has 76.6% and 74.0% identity for the α and β chains, respectively.

Mouse Hb crystallized in the orthorhombic space group $P2_12_12_1$; the crystals diffracted to 2.8 Å resolution and had unit-cell parameters a = 53.08, b = 65.94, c = 150.93 Å. Evaluation of the crystal-packing parameters indicated that the lattice accommodated one whole molecule (tetramer) in the asymmetric unit, with a solvent content of 41.62% (Matthews, 1968). The final refined model of mouse Hb had an R factor of 24.26% (R_{free} = 30.56%). The Ramachandran plot showed that 90.0%, 8.6%, 1.4% and 0% of the residues are in the most favorable, additionally allowed, generously allowed and disallowed regions, respectively. The coordinates of the final refinement have been deposited in the PDB as entry 3hrw. The structure of mouse Hb is composed of an $\alpha\beta$ dimer containing all 141 and 146 residues of the α and β subunits, respectively, as shown in Fig. 2(*a*). Mouse Hb was found to be in the met form as shown by the special environment of the porphyrins and Fe atoms without any ligands, which are well defined by the electron-density map. The secondary- and quaternary-structural features of mouse Hb differ from those of human Hb, consisting of six and seven helices linked by loops in the α and β chains. The secondary-structure composition of the α chains of mouse Hb is similar to that of the α chains of DMouse Hb, except for residues 76–82, which were not assigned as a helical structure in mouse Hb. On the other hand, the β chains of mouse Hb contained five helices that are shorter in length by one or two amino acids when compared with DMouse Hb. Also, no helical structure is found at residues 81–90 in the β chains of mouse Hb, while DMouse Hb has a helix (Inoguchi *et al.*, 2013). The $2F_o - F_c$ map at 1.0σ cutoff shows continuous electron density for both the main-chain and side-chain atoms of the entire polypeptide chain in the tetrameric mouse met Hb structure.

Tetrameric, dimeric and single α and β subunits of the mouse, human and other small animal Hbs were compared and are shown in Figs. 2(*b*)–2(*e*). The corresponding root-mean-square deviations (r.m.s.d.s) of each species are listed in Supplementary Tables S3 and S4. Similarly, structural superimposition of mouse met Hb with human Hb and with other small animal Hbs in different states, liganded (oxy R and carboxy R) and unliganded (deoxy T, met R, aquo-met R and met R2), was carried out. The r.m.s.d values were calculated based on the alignment of C$^\alpha$ atoms. Mouse met Hb showed lowest r.m.s.d. values of 0.615 Å (for 521 C$^\alpha$ atoms) and 0.904 Å (for 540 C$^\alpha$ atoms) in the tetrameric form, and 0.535 Å (for 252 C$^\alpha$ atoms) and 0.572 Å (for 260 C$^\alpha$ atoms) in the dimeric form, with R-state DMouse aquo-met Hb and human oxy Hb, respectively. Mouse met Hb exhibited an r.m.s.d. of 0.938 Å (for 540 C$^\alpha$ atoms) with tetrameric human carboxy R-state Hb. Likewise, the dimeric form of mouse met Hb exhibited r.m.s.d. values of 0.556 Å (for 226 C$^\alpha$ atoms) with APika Hb, 0.572 Å (for 260 C$^\alpha$ atoms) with human oxy R-state Hb and 0.622 Å (for 266 C$^\alpha$ atoms) with human carboxy R-state Hb. As pointed out earlier, the amino-acid sequence of guinea pig Hb differs from those of the other organisms to a greater extent, but its structural integrity was found to be similar to human Hb and other small animal Hbs, with the exception of cat Hb.

3.2. $\alpha1\beta2$ interface region

Baldwin & Chothia (1979) were the first to characterize the $\alpha1\beta2$ interface consisting of both switch and joint regions. The transition between T and R quaternary forms resulted in significant changes in the relative positions of the residues in the switch region, while the residue positions in the joint region remained relatively unchanged. In terms of inter-subunit interactions, the switch region(s) in the $\alpha1\beta2$ interface serves as an indicator of the quaternary state of the hemoglobin molecule. In mouse met Hb, the residues in the switch region(s) of the $\alpha1\beta2$ interface (β2Leu96–β2Asn102 and α1Leu91–α1Val96) were compared with those in human Hb and other small animal Hbs. The results showed a similar structural orientation of DMouse aquo-met, human carboxy and human oxy R-state Hbs, with lowest r.m.s.d values of 0.282, 0.488 and 0.532 Å, respectively (Supplementary Table

S5; Fig. 3). In the overall superposition, the switch region of mouse met Hb showed a very similar alignment of backbone and side chains to the R-state structures, except for the cat and human deoxy T-state Hbs. The backbone of human deoxy T-state Hb shifted towards β2His97 in the overlapped structure of switch regions, as shown in Fig. 3(*a*).

The switch-region β2His97 residue of T-state Hb is positioned between α1Pro44 and α1Thr41, whereas in the R-state β2His97 is repositioned between α1Thr38 and α1Thr41 due to the transition from the T- to the R-state, with a hydrogen bond between β2His97 and α1Thr38 (Shaanan, 1983). β2His97 is a key residue confirming the transition from the R- to the T-

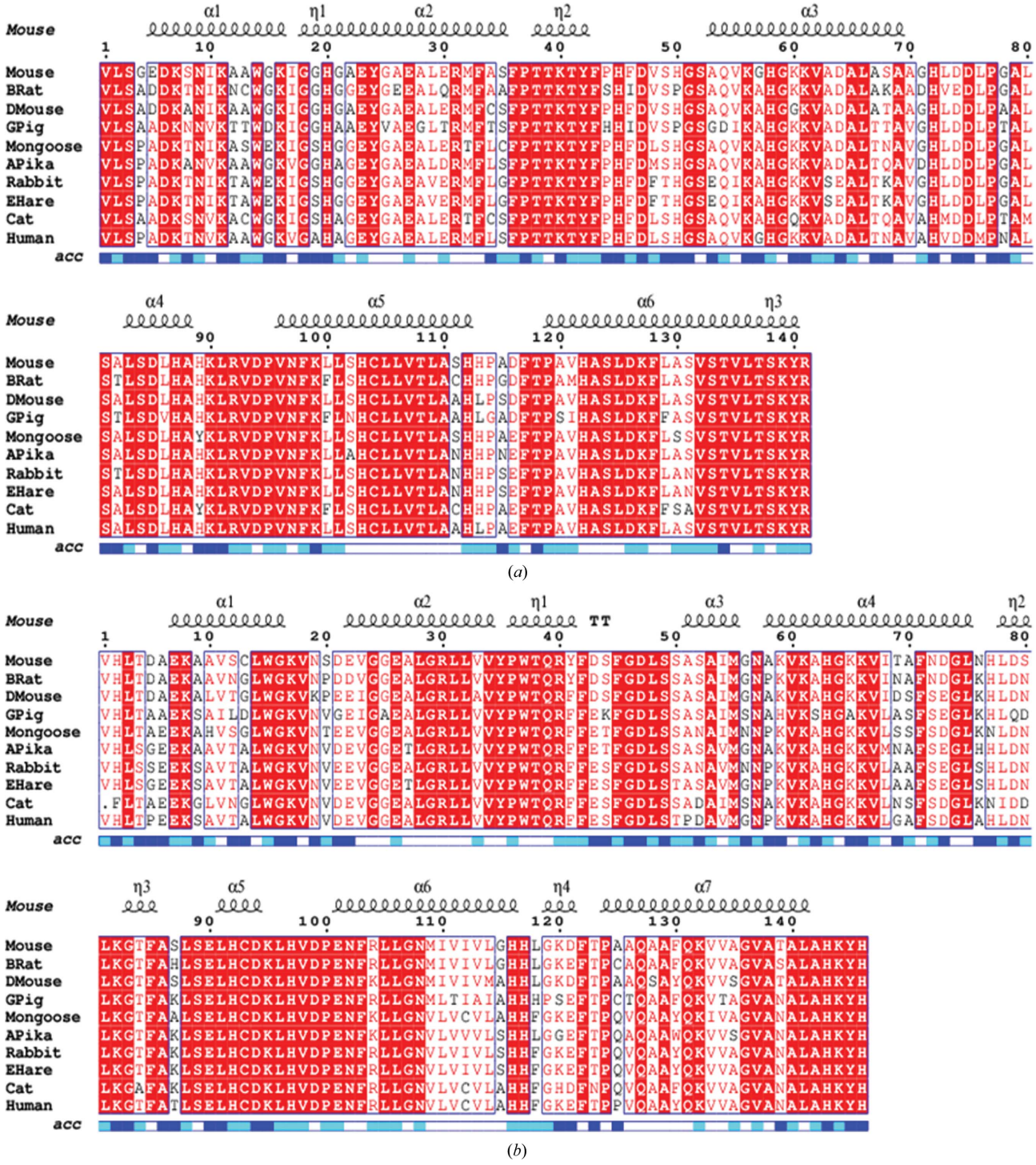

Figure 1
Multiple sequence alignment of mouse Hb with human Hb and other small animal Hbs. (*a*) Alignment of α chains and (*b*) alignment of β chains. The conserved and nonconserved residues are highlighted with red and white backgrounds, respectively. α, α-helix; η, 3_{10}-helix; TT, β-turn. A dot within the sequence represents a gap at the respective position in the corresponding species. A bar below the sequence shows the solvent accessibility of each amino acid, with blue, cyan and white representing accessible, intermediate and buried, respectively.

state with respect to its position and location in the $\alpha1\beta2$ interface of the quaternary structure. In mouse met Hb $\beta2$His97 is not positioned between $\alpha1$Thr41 and $\alpha1$Pro44 in the $\alpha1\beta2$ interface region, revealing that it does not belong to the T-state (Fig. 3*b*). $\beta2$His97 is positioned between $\alpha1$Thr38 and $\alpha1$Thr41, with three hydrogen bonds formed between $\beta2$His97 and $\alpha1$Thr41, with distances of 2.80 Å for the CB atom, 2.78 Å for the CG atom and 3.02 Å for the CD2 atom of $\beta2$His97 to the OG1 atom of $\alpha1$Thr41, as shown in Fig. 3(*b*). Also, the OG1 atom of $\alpha1$Thr41 forms three nonbonded contacts with the remaining atoms (NE2, CE1 and ND1) of the side chain of $\beta2$His97, with distances of 3.86, 4.12 and 3.56 Å, respectively. Superpositions of the switch regions of mouse met Hb with those of human oxy R-state and deoxy T-state Hb are clearly shown, with the boundaries in different colors; cyan and red represent the R- and T-states of human Hb, respectively. The reference residues $\beta2$His97 of the human Hbs are positioned within the boundaries drawn for the R- and T-state structures. In mouse met Hb, $\beta2$His97 moves towards the T-state and is located at the midpoint of the T- and R-states, which makes $\beta2$His97 form three hydrogen bonds (a hydrogen bond is in fact only possible in the R-state) and three nonbonded contacts with the OG1 atom of $\alpha1$Thr41. In human deoxy T-state Hb, there is a unique hydrogen bond between $\alpha1$Asn97 and $\beta2$Asp99 in the switch region with a distance of 2.81 Å, which is also present in mouse met Hb with a distance of 3.49 Å, clearly illustrating that the quaternary structure is moving towards the T-state (Fig. 3*b*).

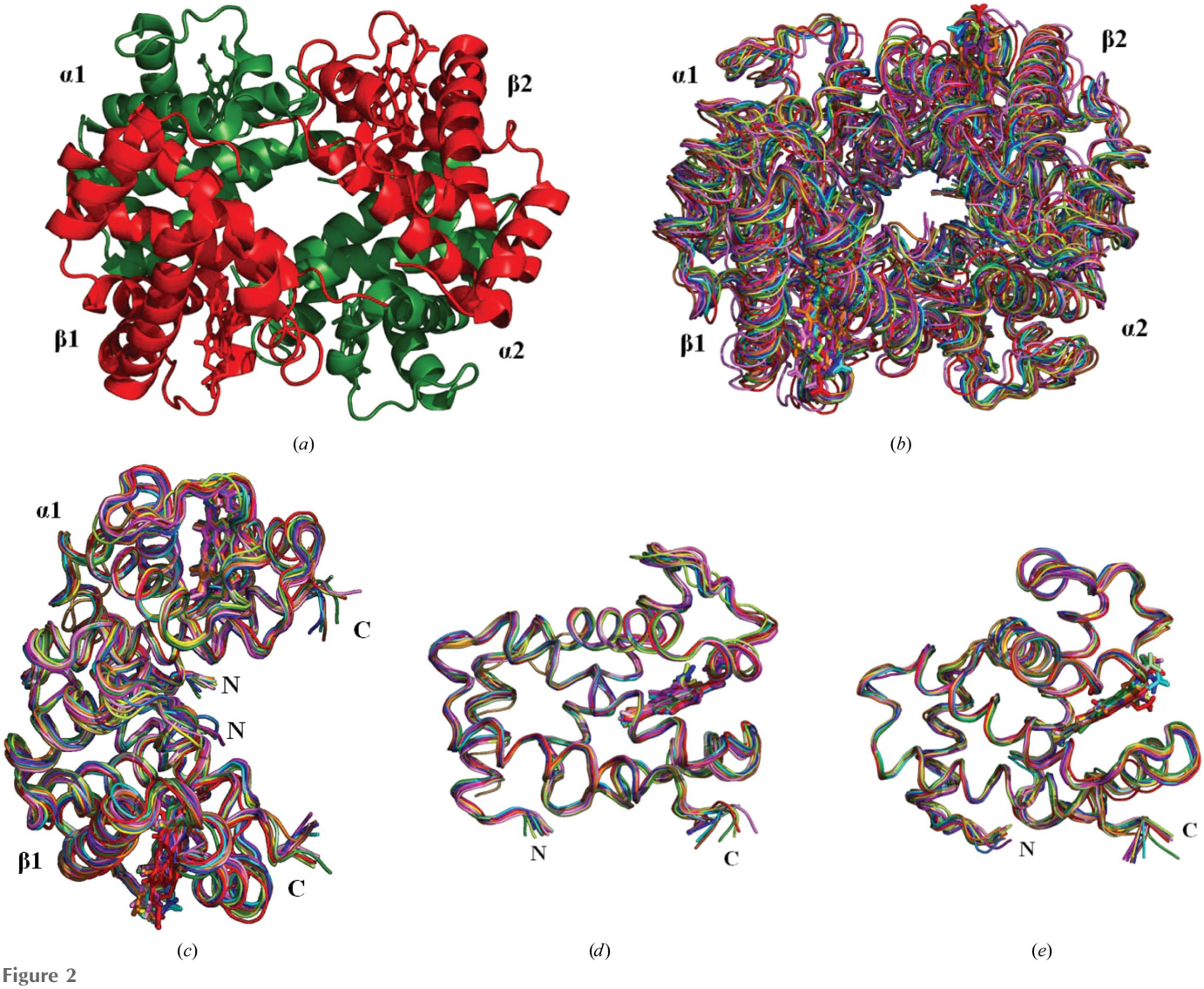

Figure 2
(*a*) Cartoon representation of the crystal structure of mouse met Hb. Structural superposition of the C^{α} traces of mouse Hb with other small animal Hbs and human Hb are shown for the tetramer (*b*), $\alpha1\beta1$ dimer (*c*), α chains (*d*) and β chains (*e*). The superimposed molecules are shown as ribbon diagrams in forest green (mouse Hb), orange (BRat Hb; PDB entry 3hf4), lemon (DMouse aquo-met Hb; PDB entry 4h2l), pale green (DMouse deoxy Hb; PDB entry 5ker), sky blue (GPig oxy Hb; PDB entry 3a0g), purple (GPig met Hb; PDB entry 3hyu), yellow (mongoose oxy Hb; PDB entry 4yu4), sand (APika Hb; PDB entry 5eui), magenta (rabbit oxy Hb; PDB entry 2rao), pink (EHare oxy Hb; PDB entry 3lqd), violet (cat Hb; PDB entry 3gqp), cyan (human oxy Hb; PDB entry 1hho), blue (human carboxy Hb; PDB entry 1aj9), red (human deoxy Hb; PDB entry 2hhb) and brown (human met Hb; PDB entry 1jy7). The heme groups of each subunit are shown in stick representation in all of the diagrams.

The C^{α} distance between β2His97 and α1Thr38 is 5.19 Å in R-state human Hb and 8.93 Å in T-state human Hb, whereas in mouse met Hb this distance is about 6.24 Å. Similarly, the C^{α} distance between β2His97 and α1Thr41 in mouse met Hb is 6.49 Å, which is an intermediate value between 7.28 Å in R-state human Hb and 4.73 Å in T-state human Hb. The appreciable variation in the distances from β2His97 to α1Thr38 and α1Thr41 shows that mouse met Hb adopts a structure that is considerably different from those of the classical R- and T-states of human Hb. These deviations in the

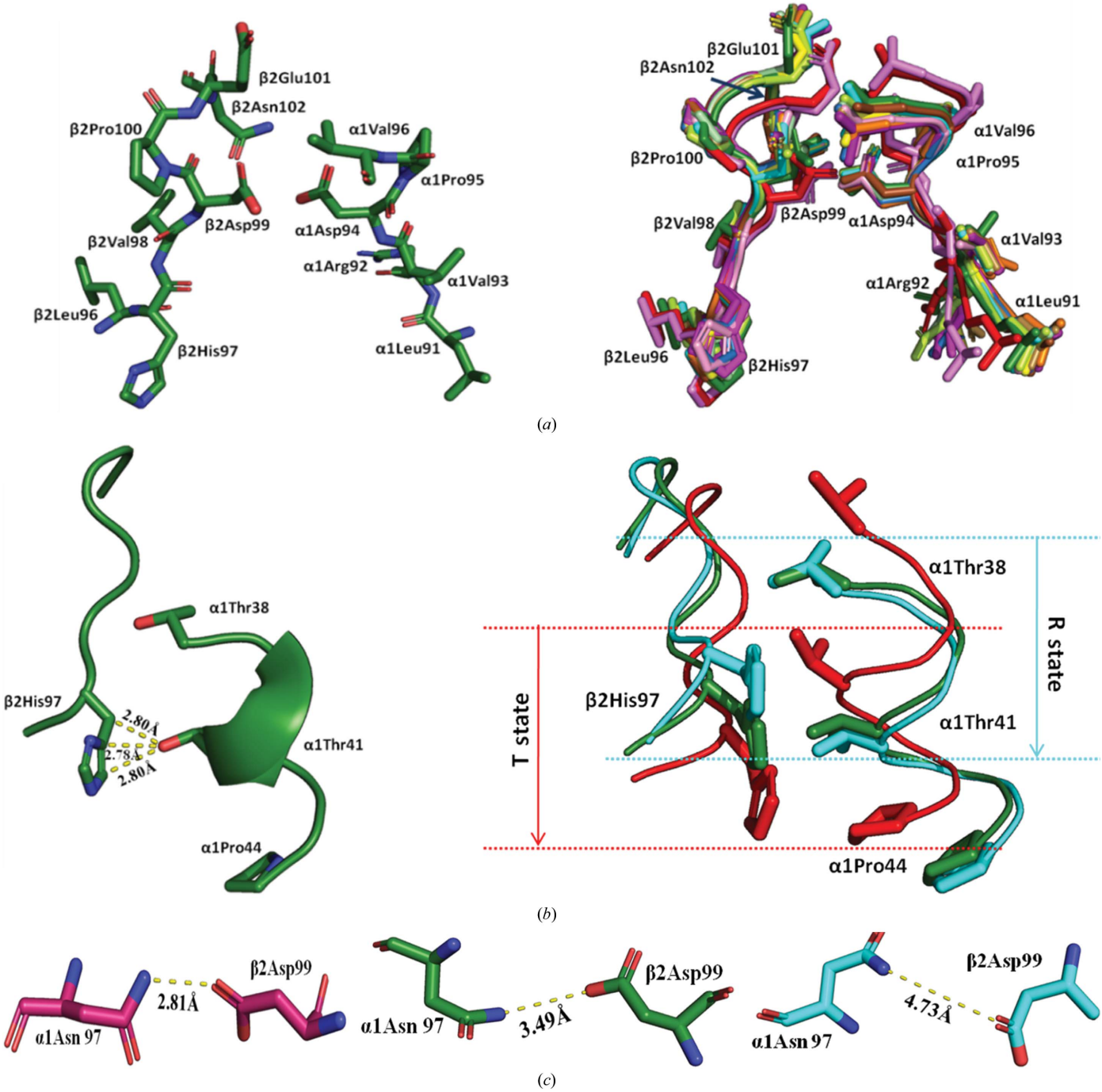

Figure 3
(*a*) Switch-region residues of mouse met Hb (left) and their alignment in human Hb and Hbs from other small animals in different colors (right). The superimposed molecules are shown as ribbon diagrams with side chains for each amino acid shown as sticks in forest green (mouse Hb), orange (BRat Hb), lemon (DMouse aquo-met Hb), pale green (DMouse deoxy Hb), sky blue (GPig oxy Hb), purple (GPig met Hb), yellow (mongoose oxy Hb), sand (APika Hb), magenta (rabbit oxy Hb), pink (EHare oxy Hb), violet (cat Hb), cyan (human oxy Hb), blue (human carboxy Hb), red (human deoxy Hb) and brown (human met Hb). (*b*) The position of the histidine residue of mouse met Hb (left) and its overlap with oxy R-state (cyan) and deoxy T-state (red) human Hbs showing the boundary lines with respect to state (right). Yellow dashed lines represent hydrogen bonds or the distances between corresponding atoms. (*c*) A unique hydrogen-bond interaction in deoxy T-state human Hb (left), in mouse met Hb (middle) and the distance between the corresponding atoms in human R-state Hb (right).

C^{α}–C^{α} distances of β2His97 from α1Thr38 and α1Thr41 in the $\alpha1\beta2$ switch region reveals that mouse met Hb is intermediate between the R- and T-states, but much closer to the R-state.

3.3. Heme analysis

In mouse Hb, the Fe atoms in all of the heme groups were well coordinated by a porphyrin ring and two proximal histidine residues without any ligands (O_2/CO/H_2O), confirming the met form of the molecule, and are well defined by $2F_o - F_c$ electron density. The heme groups of mouse met Hb and their environmental residues are shown as $2F_o - F_c$ electron-density maps in Fig. 4. The heme geometry of the α- and β-subunit heme groups in mouse met Hb were compared with a set of Hb structures from selected species previously published in different states such as DMouse Hb [deoxy T-state (PDB entry 5ker) and aquo-met R-state (PDB entry 4h2l)], guinea pig met R2-state Hb (PDB entry 3hyu) and human Hb [oxy R-state (PDB entry 1hho), carboxy R-state (PDB entry 1aj9), deoxy T-state (PDB entry 2hhb) and met R2-state (PDB entry 1jy7)] as reported in Table 2 (Inoguchi *et al.*, 2013, 2017; Pairet & Jaenicke, 2010; Shaanan, 1983; Vásquez *et al.*, 1998; Fermi *et al.*, 1984; Biswal & Vijayan, 2001). From the heme geometry, the distances between Fe and

Table 2
Geometry of the heme groups and their environment in mouse, human, DMouse and GPig Hbs.

	Mouse met		DMouse aquo-met R		DMouse deoxy T		GPig met R2		Human oxy R		Human carboxy R		Human deoxy T		Human met R2	
	α1	β1	α1	β1	α1	β1	α1	β1	α1	β1	α1	β1	α1	β1	α1	β1
Fe–His (F8) NE2 (Å)	2.10	1.82	2.24	2.26	2.50	2.56	1.98	1.99	1.94	2.07	1.93	2.16	2.15	2.15	2.35	2.47
Fe–His (E7) NE2 (Å)	4.19	3.93	4.17	4.14	4.23	4.05	4.23	4.31	4.31	4.19	4.47	4.19	4.50	4.14	5.19	4.24
Fe–Val (E11) CG2 (Å)	5.70	4.25	4.99	4.72	4.85	4.40	4.84	4.77	4.79	4.66	5.06	5.16	5.23	4.12	4.98	4.83
Fe–Phe (CD1) CZ (Å)	5.15	6.05	5.41	5.74	5.18	5.56	5.15	5.40	5.51	5.66	5.52	5.66	5.98	6.74	5.34	5.18
His (E7) NE2–Fe–His (F8) NE2 (°)	149.3	112.8	154.9	151.2	131.2	135.9	153.9	148.8	147.9	137.8	146.6	140.0	159.8	149.4	122.6	134.2
Fe–plane distance† (Å)	0.16	0.04	0.13	0.14	0.02	0.1	0.11	0.14	0.15	0.06	0.01	0.05	0.54	0.17	0.19	0.5

† The plane is defined as the porphyrin ring atoms excluding the side chains (methyl, ethyl and acid groups) and the Fe atom.

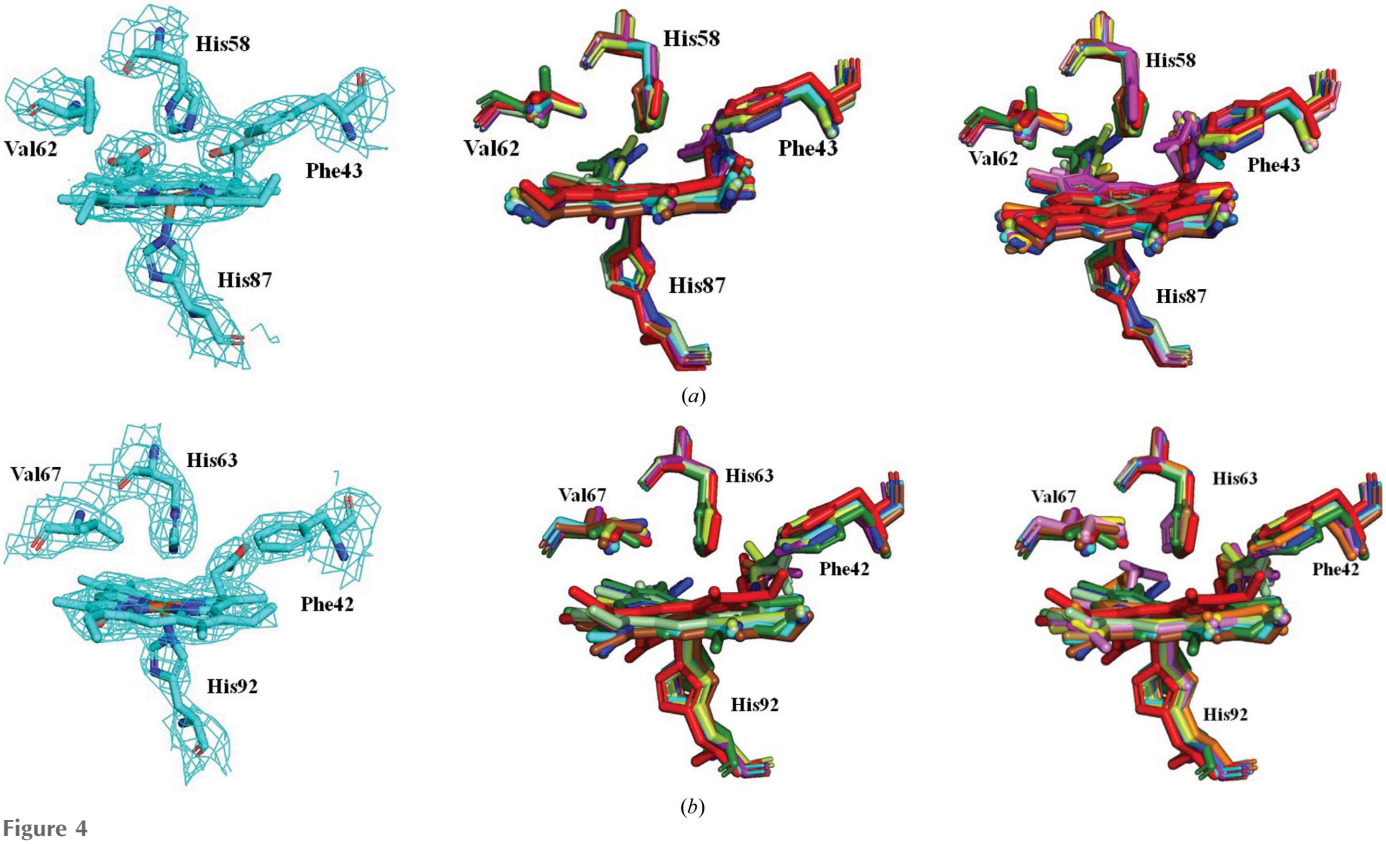

Figure 4
(*a*) Electron density for the α-heme pocket of mouse met Hb (left) and overlap diagrams for selected species (middle) and all species (right) are shown with the following coloring scheme: forest green, mouse Hb; orange, BRat Hb; lemon, DMouse aquo-met Hb; pale green, DMouse deoxy Hb; sky blue, GPig oxy Hb; purple, GPig met Hb; yellow, mongoose oxy Hb; sand, APika Hb; magenta, rabbit oxy Hb; pink, EHare oxy Hb; violet, cat Hb; cyan, human oxy Hb; blue, human carboxy Hb; red, human deoxy Hb; brown, human met Hbt. (*b*) Electron density for the β-heme pocket of mouse met Hb (left) and overlay diagrams for selected species (middle) and all species (right) are shown with the same coloring scheme as in (*a*).

βPhe42 (CD1 and CZ atoms) are 5.66 Å (oxy R- and carboxy R-states) and 6.74 Å (deoxy T-state) in human Hb, whereas in mouse met Hb the Fe to βPhe42 distance assumed an intermediate value of 6.05 Å, which is closer to the R-state conformation. The superposition of heme groups (α and β chains) of mouse met Hb with Hbs from other species is shown in Fig. 4, with the corresponding r.m.s.d. values listed in Supplementary Table S6. The α-heme group of mouse met Hb showed much smaller r.m.s.d. values with BRat Hb (0.191 Å), human carboxy R-state Hb (0.205 Å), APika Hb (0.212 Å) and human oxy R-state Hb (0.271 Å). Similarly, the mouse Hb β-chain heme group expressed a high structural resemblance to the heme groups of DMouse aquo-met R-state Hb (0.279 Å), DMouse deoxy Hb (0.323 Å), rabbit oxy Hb (0.342 Å), APika Hb (0.348 Å), human oxy R-state Hb (0.351 Å) and human carboxy R-state Hb (0.358 Å).

The nature of allosteric transitions also led to some differences in the Fe–Fe distances and geometry of heme groups in Hb structures in different states, as listed in Supplementary Table S7. The unliganded structures exhibited longer Fe–Fe distances of 134.9 Å (human met R2-state Hb), 134.6 Å (human deoxy T-state Hb), 132.8 Å (GPig met R2-state Hb), 131.7 Å (DMouse met R-state Hb) and 130.9 Å (DMouse deoxy Hb), followed by the liganded structures of human Hbs such as carboxy and oxy R-state Hbs, with Fe–Fe distances of 130.0 and 129.5 Å, respectively. In mouse met Hb the Fe–Fe distance is 131.1 Å, which is longer when compared with human R-state Hbs and shorter than in human deoxy T-state Hb, which is again confirmation of the existence of mouse met Hb in an intermediate form between R-state and T-state Hb.

4. Summary

Mice (*M. musculus*) are small animals belonging to the rodent family that live in burrows under conditions with high CO_2 levels. Mouse Hb was purified and crystallized at physiological pH in the orthorhombic space group $P2_12_12_1$, and the crystals diffracted to 2.8 Å resolution. The structure of mouse Hb was compared with human Hb and with Hbs from other small animals in terms of primary-, tertiary- and quaternary-structural features and the $\alpha1\beta2$ interface region, and the heme environment without any ligands in all four heme groups showed that mouse met Hb is an intermediate between the R-state and the T-state that is much closer to the R-state conformation.

Acknowledgements

The authors thank the G. N. Ramachandran X-ray data collection in-house facility at the University of Madras, Chennai, India for data collection. Author contributions are are follows. Dr S. S. Sundaresan solved the structure of mouse Hb. Dr Pandian Ramesh performed an extensive analysis of the individual structural features of mouse Hb and comparative analysis with human Hb and Hbs from other small animals, conceptualized and wrote the manuscript. Ms N. Shobana and Dr T. Vinuchakkaravarthy helped in manuscript preparation. Professor M. N. Ponnuswamy and Professor Yasien Sayed reviewed the manuscript for publication. The authors declare no competing interests.

Funding information

This work was partially supported through the Global Challenges Research Fund (GCRF) through the Science and Technology Facilities Council (STFC), grant No. ST/R002754/1: Synchrotron Techniques for African Research and Technology (START). This work was supported by the CSIR (India) and UGC (India).

References

Baldwin, J. & Chothia, C. (1979). *J. Mol. Biol.* **129**, 175–220.
Bartels, K. S. & Klein, C. (2003). *The AUTOMAR Manual*, v.1.4. Norderstedt: MAR Research.
Biswal, B. K. & Vijayan, M. (2001). *Curr. Sci.* **81**, 1100–1105.
Bradford, M. M. (1976). *Anal. Biochem.* **72**, 248–254.
Davis, B. J. (1964). *Ann. N. Y. Acad. Sci.* **121**, 404–427.
Emsley, P., Lohkamp, B., Scott, W. G. & Cowtan, K. (2010). *Acta Cryst.* D**66**, 486–501.
Fermi, G., Perutz, M. F., Shaanan, B. & Fourme, R. (1984). *J. Mol. Biol.* **175**, 159–174.
Inoguchi, N., Mizuno, N., Baba, S., Kumasaka, T., Natarajan, C., Storz, J. F. & Moriyama, H. (2017). *PLoS One*, **12**, e0174921.
Inoguchi, N., Oshlo, J. R., Natarajan, C., Weber, R. E., Fago, A., Storz, J. F. & Moriyama, H. (2013). *Acta Cryst.* F**69**, 393–398.
Kennerly, T. E. Jr (1964). *Tex. J. Sci.* **16**, 395–441.
Knapp, J. E., Oliveira, M. A., Xie, Q., Ernst, S. R., Riggs, A. F. & Hackert, M. L. (1999). *J. Biol. Chem.* **274**, 6411–6420.
Laskowski, R. A., MacArthur, M. W., Moss, D. S. & Thornton, J. M. (1993). *J. Appl. Cryst.* **26**, 283–291.
Matthews, B. W. (1968). *J. Mol. Biol.* **33**, 491–497.
McCoy, A. J., Grosse-Kunstleve, R. W., Adams, P. D., Winn, M. D., Storoni, L. C. & Read, R. J. (2007). *J. Appl. Cryst.* **40**, 658–674.
McNab, B. K. (1966). *Ecology*, **47**, 712–733.
Monod, J., Wyman, J. & Changeux, J.-P. (1965). *J. Mol. Biol.* **12**, 88–118.
Mueser, T. M., Rogers, P. H. & Arnone, A. (2000). *Biochemistry*, **39**, 15353–15364.
Murshudov, G. N., Skubák, P., Lebedev, A. A., Pannu, N. S., Steiner, R. A., Nicholls, R. A., Winn, M. D., Long, F. & Vagin, A. A. (2011). *Acta Cryst.* D**67**, 355–367.
Pairet, B. & Jaenicke, E. (2010). *PLoS One*, **5**, e12389.
Perutz, M. F. (1968). *J. Cryst. Growth*, **2**, 54–56.
Ramesh, P., Sundaresan, S. S., Sathya Moorthy, P., Balasubramanian, M. & Ponnuswamy, M. N. (2013). *J. Synchrotron Rad.* **20**, 843–847.
Robert, X. & Gouet, P. (2014). *Nucleic Acids Res.* **42**, W320–W324.
Safo, M. K. & Abraham, D. J. (2001). *Protein Sci.* **10**, 1091–1099.
Safo, M. K. & Abraham, D. J. (2005). *Biochemistry*, **44**, 8347–8359.
Schumacher, M. A., Zheleznova, E. E., Poundstone, K. S., Kluger, R., Jones, R. T. & Brennan, R. G. (1997). *Proc. Natl Acad. Sci. USA*, **94**, 7841–7844.
Shaanan, H. (1983). *J. Mol. Biol.* **171**, 31–59.
Silva, M. M., Rogers, P. H. & Arnone, A. (1992). *J. Biol. Chem.* **267**, 17248–17256.
Studier, E. H. & Procter, J. W. (1971). *J. Mammal.* **52**, 631–633.
Sundaresan, S. S., Ramesh, P., Sivakumar, K. & Ponnuswamy, M. N. (2009). *Acta Cryst.* F**65**, 681–683.
Vásquez, G. B., Ji, X., Fronticelli, C. & Gilliland, G. L. (1998). *Acta Cryst.* D**54**, 355–366.
Winn, M. D., Ballard, C. C., Cowtan, K. D., Dodson, E. J., Emsley, P., Evans, P. R., Keegan, R. M., Krissinel, E. B., Leslie, A. G. W., McCoy, A., McNicholas, S. J., Murshudov, G. N., Pannu, N. S., Potterton, E. A., Powell, H. R., Read, R. J., Vagin, A. & Wilson, K. S. (2011). *Acta Cryst.* D**67**, 235–242.